J. MATER. CHEM., 1995, 5(11), 2001–2006

Preparation and Crystal Structure of $LaAl(Si_{6-z}Al_z)N_{10-z}O_z$

Jekabs Grins,[a] Zhijian Shen,[b] Mats Nygren[a] and Thommy Ekström[a]
[a] *Department of Inorganic Chemistry, Arrhenius Laboratory, University of Stockholm, S-10691 Stockholm, Sweden*
[b] *Department of Materials Science and Engineering, Zhejiang University, Hangzhou 310027, P.R. China*

A new nitrogen-rich phase has been observed to form in rare-earth-metal stabilised α-sialon preparations containing Sm and Nd. The X-ray powder pattern of this phase overlapped to a great extent that of α-sialon. Large quantities of this phase were also found in samples of the overall composition $Ln_2Al_4Si_{11}N_{18}O_4$ with Ln = Ce and La. The La compound was selected for crystal structure determination, and the obtained X-ray pattern could be indexed with an orthorhombic unit cell; $a = 9.4303(7)$, $b = 9.7689(8)$, $c = 8.9386(6)$ Å. A structural model was refined in the space group *Pbcn* using the Rietveld method. Based on 267 theoretical reflections in the 2θ range 10–82°, the following *R*-values were obtained for the composition $LaAl(Si_{6-z}Al_z)N_{10-z}O_z$ with $z = 1$; $R_{wp} = 1.8$, $R_I = 6.6$ and $R_F = 5.1\%$. The Al atoms and the (Si,Al) atoms are tetrahedrally coordinated by (N,O) atoms, yielding an $Al(Si,Al)_6(N,O)_{10}^{3-}$ network. The La atoms are found in tunnels extending along the [001] direction and are irregularly coordinated by seven (N,O) atoms. The structure of this phase contains structural fragments which show strong similarities with some present in $LaSi_3N_5$; their compositional relationship is evident if their chemical formulae are expressed as $LaN–AlN–2(Si,Al)_3(N,O)_4$ and $2LaN–2Si_3N_4$.

Recent studies by us and others concerning the thermal stability of the α-sialon phase in various Me–Si–Al–O–N systems have shown that the α-sialon phase is formed at elevated temperatures but decomposes at lower temperatures, yielding an Me-rich intergranular phase.[1–5] In connection with these studies we have prepared a great number of samples along the tie-line between Si_3N_4 and $Ln_2O_3{\cdot}9AlN$, with Ln = Yb, Y, Dy, Sm and Nd, of the overall composition $Ln_xSi_{12-4.5x}Al_{4.5x}O_{1.5x}N_{16-1.5x}$ and with $0.25 \leqslant x \leqslant 1.0$. In order to reveal the true phase relationships at high temperatures it was found necessary to quench the samples rapidly, *i.e.* by applying cooling rates exceeding 400 °C min^{-1}. In the systems with Ln = Nd and Sm and for $x > 0.6$ we observed a new intergranular phase (termed the JEM phase) and elemental analysis indicated that the Ln : Si : Al atomic ratio was in the range 13 : 65 : 22.[3,4] The JEM phase was formed in conjunction with α-sialon in comparatively large amounts in the Nd system and in minor amounts in the Sm system. The JEM phase is, however, not formed in the Y, Dy and Yb systems, indicating that it is stable only for Ln ions with ionic radii larger than that of dysprosium. Note that the X-ray powder pattern of the JEM phase resembles and overlaps that of α-sialon.

Microstructural investigation in a scanning electron microscope showed that this phase was not evenly distributed in the matrix but confined to certain parts. The 'flower-like' morphology of these areas resembled to a great extent that previously found in β-sialon materials prepared with La_2O_3 as sintering aid.[6,7] In the latter system very few areas of this type appeared, and their size was too small to allow a reliable determination of the elemental content; however, the observed contrast indicated that they should be rather rich in La.

Subsequent studies have shown that the JEM phase is formed when La and Ce are used as the rare-earth metal (see below). So far we have not been able to prepare monophasic JEM samples but La and Ce samples containing 75–80% of this phase and 20–25% of β-sialon have been prepared, whereas with Ln = Nd and Sm α-sialon and melilite were always found in conjunction with the JEM phase. In this article we report on the preparation and thermal stability of the JEM phase and on the structure of the La modification as determined by Rietveld refinement based on X-ray powder diffraction (XRPD) data.

Experimental

Originally, the JEM phase was found to coexist with Nd- and Sm-doped α-sialons with overall compositions of $Ln_xSi_{12-4.5x}Al_{4.5x}O_{1.5x}N_{16-1.5x}$ for $x \geqslant 0.6$; the amount of the JEM phase increased with increasing *x*. Elemental analysis in a scanning electron microscope (SEM) equipped with an electron dispersive spectrometer (EDS) indicated that the Ln : Si : Al atomic ratio in the JEM phase was in the region of 13 : 65 : 22. Samples with a fixed Ln : Si : Al ratio ($Ln_2Al_4Si_{11}$, with Ln = Nd, La and Ce) but with different N/(O + N) contents were prepared using Si_3N_4 (UBE, SN-E10), AlN (H. C. Starck-Berlin, grade A), Al_2O_3 (Alcoa, A16SG) and La_2O_3, Ce_2O_3, Nd_2O_3 (99.9%, Johnson Matthey Chemicals Ltd.) as starting materials. The rare-earth-metal oxides were calcined at 1000 °C for 2 h before use. The starting mixtures were milled in water-free propanol for 24 h in a plastic jar, using sialon milling media. Pellets of dried powders were hot pressed (HPed) in BN-coated graphite dies in the temperature range 1650–1800 °C (25 MPa, 2 h) in a graphite resistance furnace under a protective nitrogen atmosphere. Selected samples were then heat-treated at 1650 °C for 24 h.

The densities of the sintered specimens were measured using Archimedes' principle. The crystalline phases were characterised by their X-ray powder patterns obtained in a Guinier–Hägg focusing camera with Si as internal standard. The X-ray films were evaluated using the computer-linked SCANPI system.[8] In the semi-quantitative estimation of the amounts of crystalline phases, the integrated intensities of the following reflections were used: (102) and (210) of the α-sialon, (101) and (210) of the β-sialon, (211) of the Nd-melilite phase, and (221) and (131) of the JEM phase. The relative weight fraction of each phase was then calculated from the expression:

$$W_k = I_k / \sum_{i=1}^{n} I_i;\ 1 \leqslant k \leqslant n \qquad (1)$$

where W_k is the weight fraction of phase *k*, and *n* is the number of crystalline phases present.

The surfaces of hot-pressed samples were carefully polished using standard diamond polishing techniques and furnished with a carbon coating before being examined in a scanning electron microscope (JEOL JSM 820, equipped with a Link AN 10000 EDS analyser). The actual Si, Al and Ln (Ln = La, Ce and Nd) contents of selected samples were determined by

EDS analysis using calibration curves, the final result being a mean of at least five of the experimental points determined. The micrographs given below were obtained in back scatter electron (BSE) mode.

Rietveld refinements were performed using a local version of the DBW.2S Rietveld refinement program[9] and XRPD data collected in symmetric transmission mode with a STOE STADI/P diffractometer using Cu-Kα_1 radiation. The step length was 0.02° and the 2θ range 10–82° was covered.

Results and Discussion

Phase Analysis and Microstructure

The highest JEM-phase content was found in the samples with an overall composition of $Ln_2Al_4Si_{11}N_{18}O_4$.

The results of the phase analysis are summarised in Table 1, which shows that the JEM phase coexists with β-sialon in La- and Ce-doped systems and with α-sialon and melilite in the Nd-doped system. The latter observation is in agreement

Table 1 Crystalline phase composition and densities of the prepared samples with an overall composition of $Ln_2Al_4Si_{11}N_{18}O_4$

overall composition	preparation conditions	density/g cm^{-3}	phase composition (%)			
			α	β	JEM	M
$La_2Al_4Si_{11}N_{18}O_4$	1800 °C, HPed	3.652	—	31.7	68.3	—
$Ce_2Al_4Si_{11}N_{18}O_4$	1800 °C, HPed	3.658	—	28.8	71.2	—
$Nd_2Al_4Si_{11}N_{18}O_4$	1800 °C, HPed	3.732	44.5	—	43.9	11.6
$Nd_2Al_4Si_{11}N_{18}O_4$	1725 °C, HPed	3.777	29.1	—	58.0	12.9
$Nd_2Al_4Si_{11}N_{18}O_4$	1650 °C, HPed		26.6	—	64.7	8.7

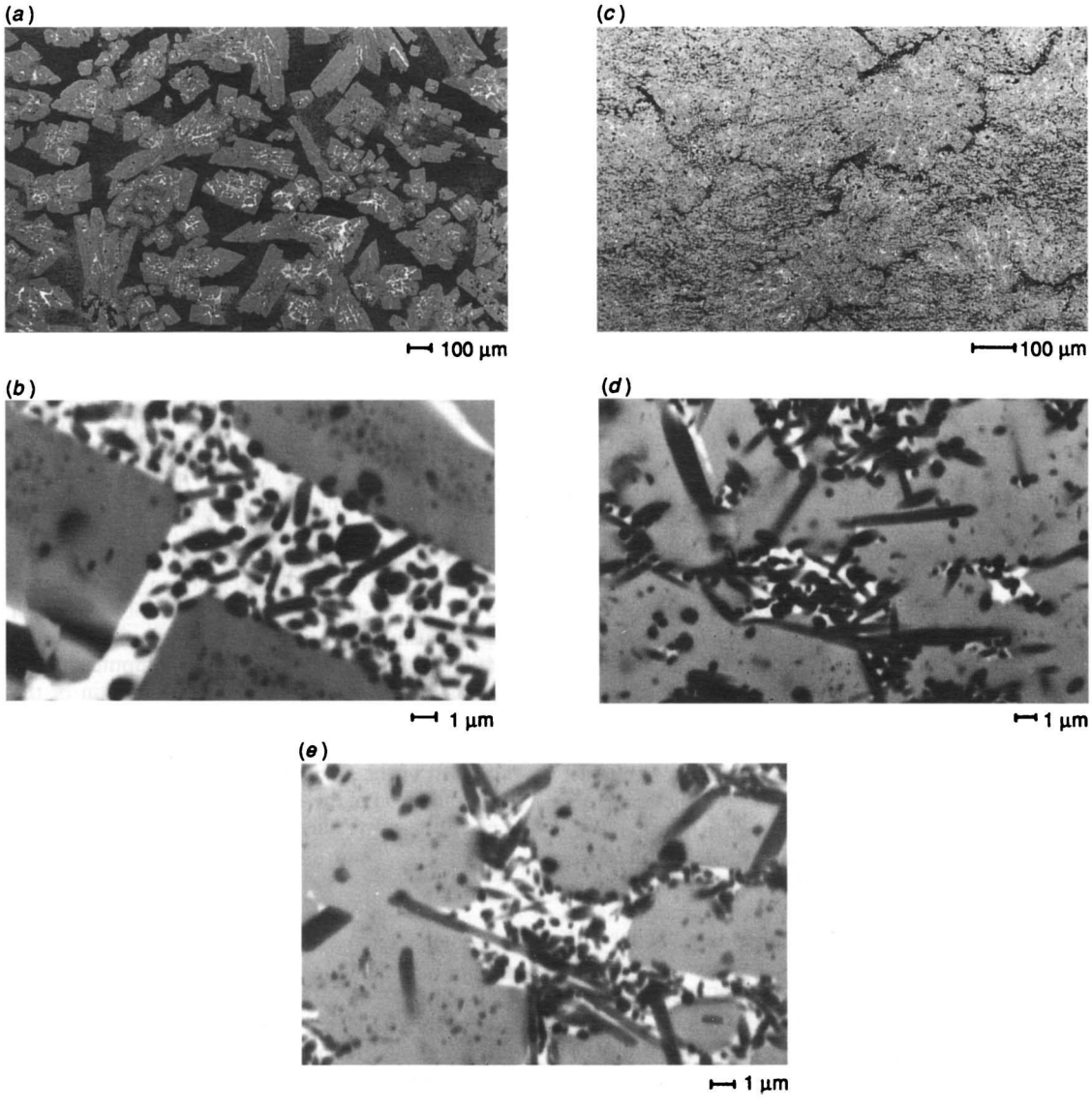

Fig. 1 SEM images of $Ln_2Al_4Si_{11}N_{18}O_4$ samples with Ln = Nd (*a*), (*b*); Ln = La (*c*), (*d*); and Ln = Ce (*e*)

with the previous findings that the JEM phase coexisted with Ln-doped α-sialon and melilite in samples with overall x values larger than 0.6 for $Ln_xSi_{12-4.5x}Al_{4.5x}O_{1.5x}N_{16-1.5x}$ compositions with Ln = Nd and Sm.[3,4]

The SEM images of the $Ln_2Al_4Si_{11}N_{18}O_4$ samples given in Fig. 1(*a*)–(*e*) show that the JEM phase tends to segregate into certain areas in the case of Ln = Nd [Fig. 1(*a*)], while for Ln = La [Fig. 1(*c*)] and Ce the JEM phase is more uniformly distributed. However, within the JEM-phase areas one can see domains of a rare-earth-metal rich phase which, in turn, contain α-sialon crystals according to X-ray and EDS analysis in the case of Ln = Nd, while for Ln = La and Ce, β-sialon crystals are formed. Note that the sialon crystals are mainly located in the rare-earth-metal rich phase areas in the Nd case [Fig. 1(*b*)], while for Ln = La and Ce, the β-sialon crystals are also found rather frequently in the JEM-phase area [Fig. 1(*d*) and (*e*)].

Structure Determination and Refinement

The La modification of the JEM phase was used for the structure determination. The powder pattern of the JEM phase was indexed with an orthorhombic unit cell, using the TREOR90 version of the indexing program TREOR.[10] The cell dimensions $a = 9.4303(7)$, $b = 9.7689(8)$, $c = 8.9386(6)$ Å, $V = 823.5$ Å^3, were obtained from Guinier-Hägg data, using Si as an internal standard and 82 reflections for $2\theta < 75°$. The indexed powder pattern is given in Table 2 for the first 20 observed lines. Note that the powder pattern severely overlaps that of α-sialon.[11]

Systematic absences in the powder pattern ($0kl$, $k \neq 2n$; $h0l$, $l \neq 2n$; $hk0$, $h+k \neq 2n$) indicated the space group *Pbcn* (no. 60). The structure was solved by the following trial and error strategy. Different arrangements were tried of six to eight equally heavy 'Al' atoms, with reasonable interatomic distances, in the asymmetric unit of the cell. The positions of these atoms were allowed to refine with a strongly damped relaxation factor, and their site occupancy factors (SOFs) were then refined together with one overall temperature factor.

Table 2 Observed and calculated 2θ values for the Guinier-Hägg diffraction pattern of $LaAl(Si_{6-z}Al_z)(N_{10-z}O_z)$ up to the 20th observed line[a]

hkl	$2\theta_{obs.}$/degrees	$\Delta 2\theta$	$d_{obs.}$/Å	I/I_0
1 1 0	13.043	0.005	6.78	31
1 1 1	16.395	0.006	5.40	38
2 0 0	18.819	0.015	4.712	8
0 0 2	19.854	0.005	4.468	5
0 2 1	20.707	0.001	4.286	12
1 1 2	23.825	0.004	3.732	40
0 2 2	27.006	−0.014	3.299	4
2 0 2	27.479	0.004	3.243	35
2 2 1	28.118	0.006	3.171	100
1 2 2	28.679	0.022	3.110	12
1 3 1	30.697	0.001	2.910	99
3 1 1	31.511	0.008	2.837	42
1 1 3	32.799	−0.004	2.728	43
2 2 2	33.123	−0.003	2.702	56
3 0 2	34.885	0.019	2.570	34
1 3 2		0.000		
3 2 1	35.380	−0.002	2.535	77
1 2 3	36.563	0.004	2.4556	60
0 4 0	36.795	0.024	2.4407	9
0 4 1	38.172	0.002	2.3558	14
2 3 2	39.177	0.009	2.2976	15

[a] $\Delta 2\theta = 2\theta_{obs.} - 2\theta_{calc.}$. $\lambda = 1.5406$ Å. Intensity values originated from diffractometer data. Cell figure-of-merit: $M_{20} = 52$, $F_{20} = 83$ (0.0074, 33).

The refined SOFs indicated which atoms were (Si,Al) and (N,O), respectively, and also which were erroneously positioned. These initial refinements furthermore indicated that the heavy La atoms were not located on any of the special positions in *Pbcn*, implying that they partially occupy a general 8(d) site. An atomic arrangement was ultimately reached, with reasonable interatomic distances and a corresponding R_F value of *ca.* 10%, which allowed the remaining (light) atoms to be located geometrically.

The obtained structural model was refined using 267 theoretical reflections for the JEM phase in the 2θ range 10–82° and the Pearson VII profile shape function. A total of 48 parameters were involved in the final refinement, including 31 positional parameters for the JEM phase. Semi-empirical correction [$\exp(-\mu R \sin\theta)$] was applied with $\mu R = 2.5$ yielding $R = 52$ μm. Collective temperature factors were used for the (Al,Si) and (N,O) atoms. The β-Si_3N_4 present in the sample was included as a second phase, with atomic coordinates from ref. 12; two cell parameters, one overall temperature factor, one unconstrained W parameter and one scale factor were refined. The R values corresponding to the final refinement are $R_{wp} = 1.8$, $R_I = 6.6$ and $R_F = 5.1\%$.

The final atomic coordinates are given in Table 3, with the estimated standard deviations (ESDs) obtained in the refinement multiplied by 2.5 in order to account for serial correlation.[13] The La atoms are found to be statistically distributed on one 8(g) site with an SOF of 0.5. Adjacent La sites are at a distance of 1.6 Å from each other (see below) and cannot therefore be simultaneously occupied. A refined value for the La SOF did not differ significantly from 0.5. The (Si,Al) atoms are found to occupy three 8(g) sites and one 4(c) site. The distribution of Si and Al on these sites cannot be discerned on the basis of the present X-ray data. The metal–anion distances for the atom on the 4(c) site are, however, found to be significantly larger than for the other (Si,Al) atoms (see below), and we therefore conclude that this site is occupied only by Al. An occupancy of only Si on the remaining 8(g) sites corresponds to a composition of $LaAlSi_6N_{10}$ for the JEM phase. EDS analyses of the JEM phase indicate a higher Al content, however, implying a composition of $LaAl(Si_{6-z}Al_z)N_{10-z}O_z$ with $z \approx 1$. The 8(g) (Si,Al) sites are therefore assumed to be partially occupied by Si and Al atoms in the ratio 5:1, and the anion sites by N and O atoms in the ratio 9:1. Note that varying z yielded no significant changes in the R values.

Structure Description

Selected bond distances and angles are given in Table 4. The Al atom and M = (Si,Al) atoms are tetrahedrally coordinated by X = (N,O) atoms. An illustration of the tetrahedral frame-

Table 3 Atomic coordinates for $LaAl(Si_{6-z}Al_z)(N_{10-z}O_z)$; space group *Pbcn*; $a = 9.4304(7)$ Å, $b = 9.7689(8)$ Å, $c = 8.9386(6)$ Å and $z = 4$; $M = (Si_{5/6}Al_{1/6})$ and $X = (N_{9/10}O_{1/10})$

atom	site	x	y	z	B/Å^2	SOF
La	8(d)	0.0553(5)	0.0961(5)	0.1824(5)	2.1(1)	0.5
Al	4(c)	0	0.427(2)	1/4	1.9(1)	1.0
M(1)	8(d)	0.434(1)	0.185(1)	0.057(1)	1.9(1)	1.0
M(2)	8(d)	0.270(1)	0.082(1)	0.520(1)	1.9(1)	1.0
M(3)	8(d)	0.293(1)	0.333(1)	0.337(1)	1.9(1)	1.0
X(1)	8(d)	0.344(2)	0.320(2)	0.140(3)	1.2(2)	1.0
X(2)	8(d)	0.383(2)	0.210(3)	0.438(3)	1.2(2)	1.0
X(3)	8(d)	0.340(2)	0.485(3)	0.410(3)	1.2(2)	1.0
X(4)	8(d)	0.110(2)	0.314(2)	0.363(3)	1.2(2)	1.0
X(5)	8(d)	0.119(3)	0.523(2)	0.127(3)	1.2(2)	1.0

Table 4 Bond distances (Å) and bond angles (degrees) in $LaAl(Si_{6-z}Al_z)(N_{10-z}O_z)$; $M=(Se_{5/6}Al_{1/6})$ and $X=(N_{9/10}O_{1/10})$

M(1)—X(1)	1.74(3)	X(1)—M(1)—X(2)	112(1)	M(2)—X(3)	1.72(3)	X(1)—M(2)—X(2)	103(1)
X(2)	1.74(3)	X(1)—M(1)—X(4)	107(1)	X(5)	1.75(3)	X(1)—M(2)—X(3)	106(1)
X(5)	1.78(2)	X(1)—M(1)—X(5)	113(1)	X(1)	1.79(3)	X(1)—M(2)—X(5)	110(1)
X(4)	1.78(3)	X(2)—M(1)—X(4)	105(1)	X(2)	1.80(3)	X(2)—M(2)—X(3)	121(1)
mean	1.76	X(2)—M(1)—X(5)	113(1)	mean	1.77	X(2)—M(2)—X(5)	106(1)
		X(4)—M(1)—X(5)	106(1)			X(3)—M(2)—X(5)	111(1)
M(3)—X(3)	1.68(3)	X(1)—M(3)—X(2)	109(1)	Al—X(5)	2 × 1.83(3)	X(4)—Al—X(4)	105(2)
X(2)	1.73(3)	X(1)—M(3)—X(3)	111(1)	X(4)	2 × 1.83(3)	X(4)—Al—X(5)	2 × 107(1)
X(4)	1.75(2)	X(1)—M(3)—X(4)	113(1)	mean	1.83	X(4)—Al—X(5)	2 × 109(1)
X(1)	1.83(3)	X(2)—M(3)—X(3)	106(1)			X(5)—Al—X(5)	118(2)
mean	1.75	X(2)—M(3)—X(4)	110(1)				
		X(3)—M(3)—X(4)	108(1)				
X(1)—M(1)	1.74(3)	M(1)—X(1)—M(2)	116(2)	X(2)—M(3)	1.73(3)	M(1)—X(2)—M(2)	119(1)
M(2)	1.79(3)	M(1)—X(1)—M(3)	126(2)	M(1)	1.74(3)	M(1)—X(2)—M(3)	127(1)
M(3)	1.83(3)	M(2)—X(1)—M(3)	112(1)	M(2)	1.80(3)	M(2)—X(2)—M(3)	114(1)
La	2.88(2)			La	2.95(2)		
X(3)—M(3)	1.68(3)	M(2)—X(3)—M(3)	123(1)	X(4)—M(3)	1.75(2)	M(1)—X(4)—M(3)	111(1)
M(2)	1.72(3)			M(1)	1.78(3)	M(1)—X(4)—Al	114(1)
La	2.45(2)			Al	1.83(2)	M(3)—X(4)—Al	115(1)
La	2.51(3)			La	2.67(2)		
La	2.74(3)			La	2.72(2)		
X(5)—M(2)	1.75(3)	M(1)—X(5)—M(2)	120(1)	La—X(3)	2.45(2)		
M(1)	1.78(2)	M(1)—X(5)—Al	120(1)	X(3)	2.51(3)		
Al	1.83(3)	M(2)—X(5)—Al	113(1)	X(4)	2.67(2)		
				X(4)	2.72(2)		
				X(3)	2.74(3)		
				X(1)	2.88(2)		
				X(2)	2.95(2)		
				La—La	1.60(1)		

work $AlM_6X_{10}^{3-}$ is shown in Fig. 2(*a*). The mean Al—X and M—X distances are 1.83 and 1.76 Å, respectively. The effective ionic radii in nitrides[14] for the present atoms are $N^{3-}=1.44$ Å, $Si^{4+}=0.29$ Å and $Al^{3+}=0.41$ Å, yielding expected interatomic distances of 1.85 and 1.73 Å for pure Al—N and Si—N bonds, respectively. The La atoms are found in tunnels, extending along [001], formed by the $AlM_6X_{10}^{3-}$ framework and are irregularly coordinated by seven X atoms at an average distance of 2.70 Å [see also Fig. 2(*b*)].

The structure of the JEM phase $LaAlM_6X_{10}$ may be compared to the structure of $LaSi_3N_5$.[15,16] The La content in the JEM phase is approximately half of that in $LaSi_3N_5$, and the X-ray density of the JEM phase ($\rho_{calc.}\approx 3.8$ and $\rho_{obs.}=3.652$ g cm^{-3}) is consequently midway between the densities of β-Si_3N_4 (2.9 g cm^{-3}) and $LaSi_3N_5$ (4.6 g cm^{-3}). The compositional similarity may furthermore be accentuated by rewriting the formula of $LaSi_3N_5$ as $2LaN{-}2Si_3N_4$ and the formula of the JEM phase as $LaN{-}AlN{-}2M_3X_4$. In the $LaSi_3N_5$ structure there are two types of N environment. In one type (I), N is coordinated by three Si in an arrangement similar to that in β-Si_3N_4 and α-Si_3N_4. In the other type (II), N is surrounded by two Si and two La atoms. The charge balance towards the La atoms is thus maintained by the type II N atoms, which are proposed to play a similar role to non-bridging O atoms in silicates.[16] In the structure of the JEM phase the coordination of the X atoms by metal atoms may be summarised as:

X(1): by 3 M at an average of 1.79 Å and 1 La at 2.88 Å
X(2): by 3 M at an average of 1.76 Å and 1 La at 2.95 Å
X(3): by 2 M at an average of 1.70 Å and 3 La at an average of 2.56 Å
X(4): by (2 M + 1Al) at an average of 1.79 Å and 2 La at an average of 2.70 Å
X(5): by (2 M + 1Al) at an average of 1.79 Å

Note here that the SOF for the La sites is 0.5 and that only two out of the three La sites surrounding X(3) and only one out of the two La sites surrounding X(4) can be occupied simultaneously. The charge balance for the JEM-phase structure is more complicated than that for $LaSi_3N_5$ owing to the full occupancy of Al on the 4(c) sites and to the partial occupancy of the 8(d) site of the La atoms. The X(1), X(2) and X(5) atoms are similar to the type I N atoms in $LaSi_3N_5$ in the sense that they are mainly bonded to three (Si,Al) atoms. The local environments around X(1) and X(2) are dependent on whether or not the corresponding La sites are occupied. The charge balance towards the La atoms is achieved mainly by the X(3) atoms, which have a coordination similar to that of the type II N atoms in $LaSi_3N_5$, and to a lesser extent by the X(4) anions. In addition, the X(3) site has the lowest mean bond length to M atoms and the largest number of La neighbours and accordingly this site stands out as a candidate for oxygen occupation. However, in order to make more precise comments on the distribution of the non-metals one needs single-crystal data.

Concluding Remarks

The JEM phase discussed above is formed by a solid-state reaction between appropriate starting materials. As shown in ref. 3, the JEM phase is also formed in α-sialon-based materials during post heat-treatment in the temperature range 1500–1650 °C according to the following reaction:

$$\alpha_1 + \text{liquid} \rightarrow \alpha_2 + \text{JEM phase} \qquad \text{(I)}$$

The formation of the JEM phase consumes neodymium both from the α-sialon and the residual liquid grain-boundary phase. This leads to a change of the composition of α-sialon from being neodymium rich (α_1) to being neodymium poor (α_2). This observation and the findings in Table 1 suggest that the Nd-containing JEM phase is more stable than the Nd-containing α-sialon with high Al content at low temperatures ($T\leqslant 1700$ °C).

The formation of rare-earth-metal containing phases in different sialon systems has been extensively investigated in the past (see ref. 17, and references therein). A number of rare-earth-metal phases can thus be formed, and their structures depend not only on the rare-earth-metal used but also on the overall N/(N + O) content. The oxynitride phase with the

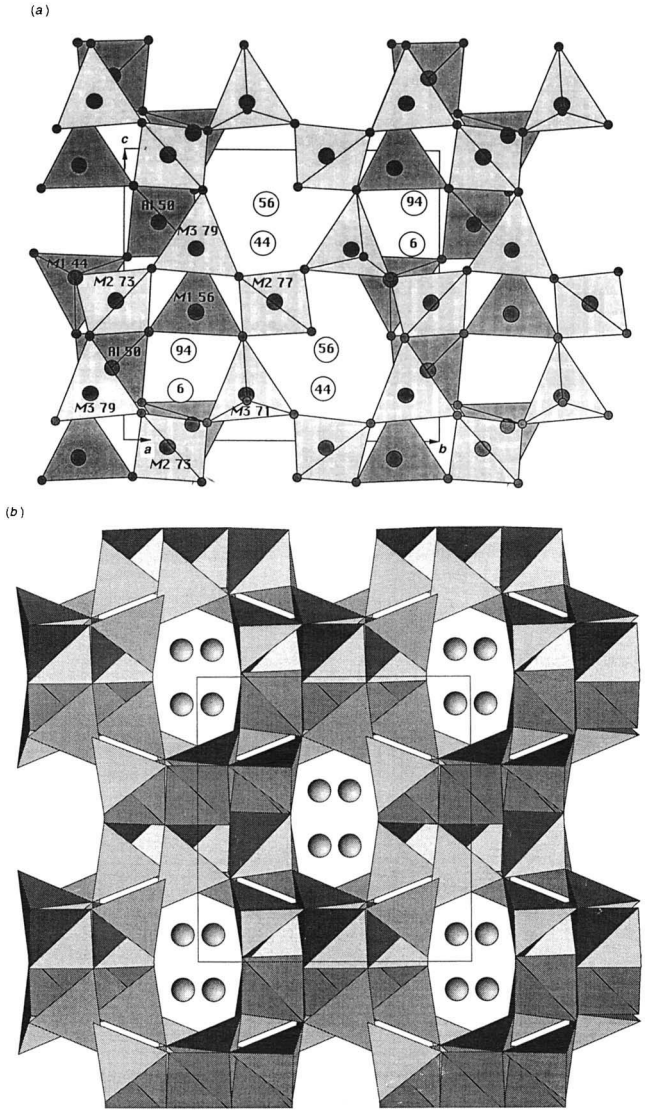

Fig. 2 (*a*) Illustration of a part of the $Al(Si_{6-z}Al_z)(NO)_{10}^{3-}$ framework projected along the [100] direction of the unit cell. Only the tetrahedra at *ca.* 3/4 and 1/2 are shown, with the numbers representing the *x*-coordinates in %. Equivalent layers of tetrahedra are found at $x \approx 1/4$ and 0, symmetry related *via* 2_1 axes parallel with the ***a*** axis. The positions of the La (Si,Al) and (N,O) atoms are shown by unfilled, medium-sized and small circles, respectively. (*b*) Structure of $LaAl(Si_{6-z}Al_z)N_{10-z}O_z$ viewed along the [001] direction of the orthorhombic unit cell. Only two of the four La positions (dashed circles) are occupied simultaneously.

highest N-content observed previously is melilite, $Ln_2Si_3O_3N_4$, which is far less N-rich than the JEM phase, having the composition $LaAl(Si_{6-z}Al_z)N_{10-z}O_z$ with $z \approx 1$. The fact that the JEM phase has not previously been observed is most probably due to the following circumstances: (i) the JEM phase is not formed in Ln–sialon systems with Ln = Yb, Y and Dy and only in limited amounts in the Sm–sialon system; (ii) it is well known that La and Ce ions cannot be accommodated in the α-sialon structure, implying that the nitrogen-rich La– and Ce–sialon compositions were not studied in great detail earlier.

In conclusion, the JEM phase forms most easily in the La–Al–Si–O–N and Ce–Al–Si–O–N systems. We intend to prepare more phase-pure materials and also to investigate the extension of the homogeneity range (*z*-value) of this phase.

Z. J. S. is thankful for a scholarship from the Swedish Institute. Financial support from the Swedish Research Council of Engineering Sciences is gratefully acknowledged.

References

1 H. Mandal, D. P. Thompson and T. Ekström, *J. Europ. Ceram. Soc.*, 1993, **12**, 421.
2 Z-J. Shen and T. Ekström, *Proc. 5th Intern. Conf. on Ceramics for Engin., Shanghai, China*, ed. D. S. Yan, X. R. Fu and S. X. Shi, World Scientific Publishing, Singapore, 1995, p. 206.
3 Z-J. Shen, T. Ekström and M. Nygren, *J. Am. Ceram. Soc.*, submitted.
4 Z-J. Shen, T. Ekström and M. Nygren, *J. Europ. Ceram. Soc.*, in the press.
5 Z-J. Shen, T. Ekström and M. Nygren, *J. Hard Mater.*, submitted.
6 P-O. Olsson and T. Ekström, *J. Mater. Sci. Lett.*, 1989, **8**, 1067.
7 P-O. Olsson and T. Ekström, *J. Mater. Sci.*, 1990, **25**, 1824.
8 K-E. Johansson, T. Palm and P-E. Werner, *J. Phys. E*, 1980, **13**, 1289.
9 D. B. Wiles, A. Sakthivel and R. A. Young, *Users Guide to Program DBW3.2S for Rietveld Analysis of X-ray and Neutron Powder Diffraction Data Patterns (Version 8804)*, School of Physics, Georgia Institute of Technology, Atlanta, 1985.
10 P-E. Werner, L. Eriksson and M. Westdahl, *J. Appl. Crystallogr.*, 1985, **18**, 367.
11 JCPDS card no. 42-251.

12 R. Grün, *Acta Crystallogr., Sect. B*, 1979, **35**, 800.
13 J-F. Berár and P. Lelann, *J. Appl. Crystallogr.*, 1991, **24**, 1.
14 W. H. Bauer, *Cryst. Rev.*, 1987, **1**, 59.
15 Z. Inoue, M. Mitomo and N. II, *J. Mater. Sci.*, 1980, **15**, 2915.
16 Z. Inoue, *J. Mater. Sci. Lett.*, 1985, **4**, 656.
17 H. Mandal, D. P. Thompson and T. Ekström, *Key Eng. Mater.*, 1992, **72–74**, 187.

Paper 5/03452C; *Received* 30*th May*, 1995